EuCARD-2

Enhanced European Coordination for Accelerator Research & Development

Journal Publication

Injection of electrons by colliding laser pulses in a laser wakefield accelerator
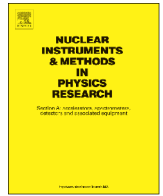
Hansson, Martin (Lund University) *et al*

26 February 2016

The electronic version of this EuCARD-2 Publication is available via the EuCARD-2 web site <http://eucard2.web.cern.ch/> or on the CERN Document Server at the following URL: <http://cds.cern.ch/search?p=CERN-ACC-2016-0347>

Injection of electrons by colliding laser pulses in a laser wakefield accelerator

M. Hansson *, B. Aurand, H. Ekerfelt, A. Persson, O. Lundh

Department of Physics, Lund University, P.O. Box 118, S-22100 Lund, Sweden

ABSTRACT

To improve the stability and reproducibility of laser wakefield accelerators and to allow for future applications, controlling the injection of electrons is of great importance. This allows us to control the amount of charge in the beams of accelerated electrons and final energy of the electrons. Results are presented from a recent experiment on controlled injection using the scheme of colliding pulses and performed using the Lund multi-terawatt laser. Each laser pulse is split into two parts close to the interaction point. The main pulse is focused on a 2 mm diameter gas jet to drive a nonlinear plasma wave below threshold for self-trapping. The second pulse, containing only a fraction of the total laser energy, is focused to collide with the main pulse in the gas jet under an angle of 150°. Beams of accelerated electrons with low divergence and small energy spread are produced using this set-up. Control over the amount of accelerated charge is achieved by rotating the plane of polarization of the second pulse in relation to the main pulse. Furthermore, the peak energy of the electrons in the beams is controlled by moving the collision point along the optical axis of the main pulse, and thereby changing the acceleration length in the plasma.

1. Introduction

The research on laser wakefield accelerators, first proposed by Tajima and Dawson [1] in 1979, has been highly active since the break-through in 2004 when it was demonstrated that laser wakefield accelerators could produce electron beams with quasi-monoenergetic spectra in the so-called bubble regime [2–4]. However, laser wakefield accelerators still suffer from several issues, and in particular large shot-to-shot fluctuations, large energy spread and divergence. One of the causes of the fluctuations is the injection and trapping of electrons, which in many experiments is achieved by self-trapping. Self-trapping occurs as the velocity of the electrons constituting the plasma wave approaches and exceeds the phase-velocity of the wave. Since the evolution of the laser pulse in the plasma and the excitation of the plasma wave is highly non-linear, both the number of trapped electrons and the final energy of the electrons tends to be hard to control. For this reason, several techniques for externally triggered injection and trapping of electrons in laser wakefield accelerators have been developed and proved to be successful to decrease shot-to-shot fluctuations and to improve the quality of the beams. These include, among others, injection in density down-ramps [5–

7] or density transitions [8,9], injection by ionization from inner shells [10,11] and injection by colliding laser pulses [12–14].

In the scheme of injection by colliding laser pulses, a focused laser pulse drives a plasma wave in its wake to a large amplitude, but below the threshold for self-trapping. A second focused counter-propagating laser pulse, with lower intensity, is spatially and temporally overlapped with the main pulse at a certain time and position in the plasma. During the collision of the two pulses, a beat-wave is formed which exerts a large ponderomotive force on the plasma electrons. For amplitudes of the two pulses over a certain threshold [14], this force stochastically heats the plasma electrons and a fraction of these electrons gain sufficiently large forward momentum to become trapped in the wake driven by the main pulse.

The technique of injection by colliding laser pulses has been shown to generate high quality beams [15–17], regarding divergence, energy spread of the quasi-monoenergetic spectra and electron pulse duration. However, this technique is experimentally challenging since two laser pulses of high intensity have to be spatially and temporally overlapped at the desired point of injection and requires high control and stability of the pointing of the two laser pulses.

In this article we report on our experiments on colliding pulse injection, and our efforts to decrease the complexity in the experimental set-up. We anticipate that such simplified set-up

* Corresponding author.
 E-mail address: martin.hansson@fysik.lth.se (M. Hansson).

allows the technique to become more approachable for further studies including studies of applications of the electron beams.

2. Experimental set-up and methods

The experiments were conducted at the Lund Laser Centre, using a multi-terawatt laser operating at 10 Hz at a central wavelength of 800 nm. The laser system produces pulses of up to 1 J after compression in a single 50 mm diameter beam. The beam position and pointing is monitored at several points in the laser system and, using piezoelectric actuated mirrors, an automated system compensates for long term drifts.

The experimental set-up is illustrated in Fig. 1(a), showing the incoming beam from the laser system from bottom left. The pulse duration is estimated from autocorrelation measurements to (40 ± 4) fs full width at half maximum (FWHM). The beam is split into two parts using a small pick-up mirror close to the interaction point. The pick-up mirror is elliptical such that it reflects a circular 1/2 in. beam perpendicular to the optical axis of the main beam. Also, the substrate of this mirror is cut to leave a circular shade in the main beam without blocking any additional part of the main beam.

The main laser beam, used for the pulses that drive the plasma wake, is focused using an off-axis parabolic mirror with an effective focal length of 750 mm. The beam reflected by the pick-up mirror is used for the pulses that trigger the injection and is focused using an off-axis parabolic mirror with an effective focal length of 100 mm. The injection pulses are focused onto the optical axis of the main beam at, or at the vicinity of, the main beam waist. The optical axes of the two focused beams are both in the horizontal plane, in which they make an angle of 150°. The beam line used for the injection pulses include a motorized linear

translation stage to move the collision point along the optical axis of the main beam, and a second motorized linear translation stage to allow for re-focusing of the injection pulses under vacuum. A manually actuated delay stage allows for coarse adjustment of the temporal overlap of the two pulses at the interaction point before the experimental chamber is pumped to vacuum. The fine adjustment is then made by a motorized linear translation stage that moves the pick-up mirror along the direction of the reflected beam. Furthermore, a rotatable zero-order mica $\lambda/2$ wave retarder is inserted, for specific data series, in the beam line and allows rotation of the plane of polarization of the injection pulses. The wave retarder is approximately 80 μm thick and is not expected to affect the duration of the injection pulses significantly. However, the transmittance of the wave retarder is measured to 0.8 and the peak intensity of the injection pulses is decreased by the same factor.

The foci of the two beams are imaged simultaneously using a microscope by reflecting the beams on the top edge of a prism, shaped to reflect both beams vertically in the direction of the microscope objective (see Fig. 1(b)). This imaging system is used to spatially overlap the two pulses, by inserting the prism edge and imaging the desired position for the collision, and then steering the two foci there. Fig. 1(c) shows a typical image of the two foci on the top edge of the prism after the spatial overlap has been tuned. In order to clearly see both foci in this figure, the normalization of the color map is different in the two regions separated by the dashed line, which also marks the position of the edge of the prism.

By fitting Gaussian distributions to the intensity distribution of each foci, the diameter (FWHM) of the foci of the main and injection beam are determined to be 20 μm and 11 μm, respectively. Furthermore, the amount of energy fitted into each Gaussian is 470 mJ and 42 mJ, respectively. Assuming a Gaussian
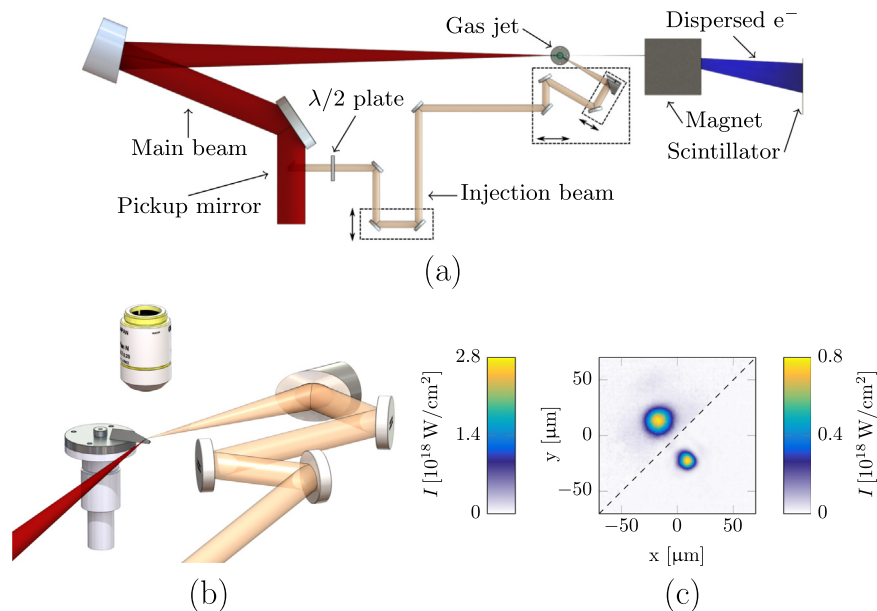

Fig. 1. (a) Schematic illustration of the experimental set up. The main beam of pulses driving the wakefield is focused using an $f = 750$ mm parabolic mirror onto a jet of hydrogen gas. The beam of pulses to trigger injection is generated using a pick-up mirror in the single beam from the laser system and is focused using an $f = 100$ mm parabolic mirror on the optical axis of the main beam close to its waist. The electrons, trapped and accelerated in the interaction in the plasma, propagate along the optical axis of the main beam out of the plasma and are dispersed by a dipole magnetic field according to energy before they impact on a scintillating screen. The pick-up mirror is mounted on a motorized linear translation stage, with the translation axis in the direction of the reflected beam, which allows for fine tuning of the temporal overlap of the pulses at the position of spatial overlap. For specific data series, a rotatable zero-order mica $\lambda/2$ wave retarder is inserted in the beam line and allows rotation of the plane of polarization of the injection pulses. (b) Imaging system used to observe the foci of the main and injection beam simultaneously. The upper edge of a prism, cut to reflect both beams vertically towards a microscope objective, is inserted at the desired position of collision. The foci of the beams are then steered to this position using motorized actuators. (c) Image acquired using the system shown in (b), showing the intensity distribution of the foci from the two pulses. Note that the scale of the color map is different for the two parts of the image. The wavefront of the laser beam is corrected using a deformable mirror. (For interpretation of the references to color in this figure caption, the reader is referred to the web version of this paper.)

distribution temporally, with the determined pulse duration, the peak intensities are 2.8×10^{18} W/cm² and 0.8×10^{18} W/cm², for the main and injection pulse respectively, corresponding to normalized vector potentials of 1.1 and 0.6.

A gas nozzle with an orifice diameter of 2 mm located approximately 1 mm from the optical axis, provides a jet of hydrogen gas with its front edge at the waist of the main beam. The neutral density distribution is characterized off-line by measuring, using a wavefront sensor, the additional optical path length introduced by the gas in an optical probe beam [18], and by assuming circular symmetry in the plane of the two laser pulses.

The accelerated electrons exit the plasma along the optical axis of the main laser pulse, and are dispersed by a dipole magnetic field before impacting on a scintillating screen. Images of the scintillating screen are acquired for each shot and are used to determine the electron energy spectra. The response of the imaging system is absolutely calibrated, which is used together with published calibration factor for the scintillating screen [19] to determine the amount of charge in the beams of accelerated electrons.

3. Results

During the experiment, the pick-up mirror is first removed from the beamline. In this case, beams of accelerated electrons are observed for electron number densities above 1.1×10^{19} cm⁻³. The beams of electrons show the typical features of self-trapped beams, with electron energy spectra containing one or more peaked features [20]. The energy value of these peaks are fluctuating from shot to shot in the range from approximately 50 MeV to 200 MeV and the amount of detected charge is of the order of 50 pC with fluctuations (standard deviation) of 50%.

The density is then lowered well below this threshold, to 8×10^{18} cm⁻³, to make sure that no accelerated electrons in the succeeding shots are due to self-trapping, and the pick-up mirror is inserted. After optimizing both spatial and temporal overlap of the main and injection pulses at the desired position of injection, quasi-monoenergetic beams of accelerated electrons with low divergence (≈ 3 mrad) are observed. These beams of accelerated electrons have a small energy spread, typically below 5 MeV (FWHM). Due to the lower peak intensity of the main pulse, the

density can be increased to 1.2×10^{19} cm⁻³, while still observing high-quality electron beams. Images of dispersed electron beams on the scintillating screen for two shots at the same plasma electron number density and with the collision point approximately in the center of the gas jet are shown in Fig. 2(a), together with the electron energy spectra for each beam. It is confirmed, by blocking the injection pulse, that no beams of accelerated electrons are generated due to self-trapping. It is observed in this figure that the beams impacting on the scintillating screen are close to circular symmetric. This suggests that the measured energy spread is most likely limited by the resolution of the electron spectrometer and divergence of the electron beams.

To confirm that the trapped charge is due to the interference of the two colliding pulses, the plane of polarization of the injection pulses is rotated. The amount of detected charge as a function of angle of rotation (θ) of the plane of polarization of the injection pulse with respect to the horizontal plane, is shown in Fig. 2(b), for a sequence of shots taken using a plasma electron number density of 1.1×10^{19} cm⁻³. Maximum amount of charge is detected with both pulses polarized in the horizontal plane ($\theta = 0°$), for which the interference between the pulses is maximal. In contrast, with the injection pulse polarized in the vertical plane, there is minimal interference between the two pulses as they cross each other, and as a result no charge is detected on any of these shots.

The energy of the accelerated electrons is controlled by changing the position of collision in the plasma along the optical axis of the main beam, while still maintaining the temporal overlap of the two pulses. This is achieved in the experiment using either of two methods. (I) By moving the translation stage holding the focusing mirror of the injection pulse, the position of collision is changed while keeping the plasma fixed with respect to the main beam focus. The drawback of this method is that both the spatial and temporal overlap had to be re-checked after every change of collision point. This prevented systematic studies of the properties of the beams as a function of collision point. (II) By instead moving the gas nozzle, the length of the remaining plasma after the collision point is thus varied. Since no fine tuning of the spatial and temporal overlap needs to be done between different positions of the plasma, this method allowed for systematic studies of the properties of the beams of accelerated electrons as a function of collision point. However, moving the plasma with respect to the
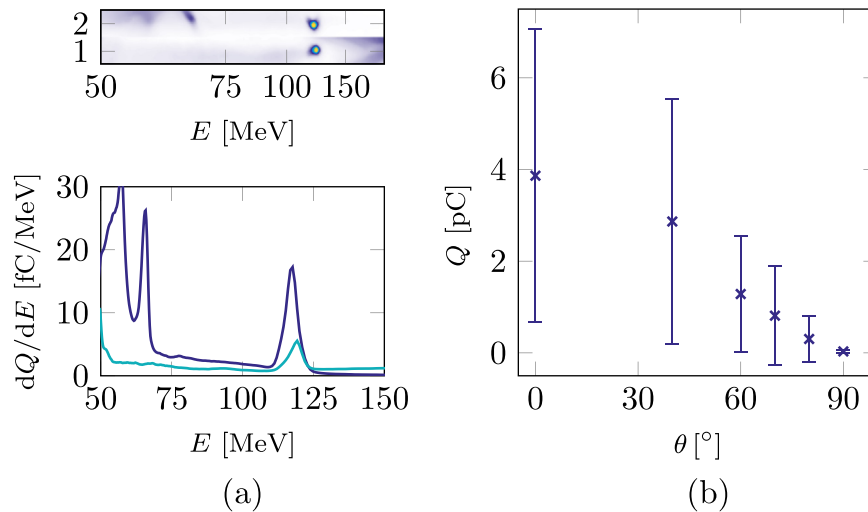

Fig. 2. (a) High quality beams of accelerated electrons, trapped by the collision of the two laser pulses in the plasma. The divergence (FWHM) of the beams is 3 mrad and the beams are quasi-monoenergetic at 120 MeV. The amount of detected charge is controlled by rotating the plane of polarization of the injection beam (b). The error bars mark the standard deviation of 10 shots. At $\theta = 0°$, the plane of polarization of the injection pulse is horizontal, which allows for maximum interference with the main pulse. At an angle $\theta = 90°$ of the plane of polarization of the injection pulse, with respect to the horizontal plane, there is no interference of the two pulses and no trapped charge is observed at this angle.
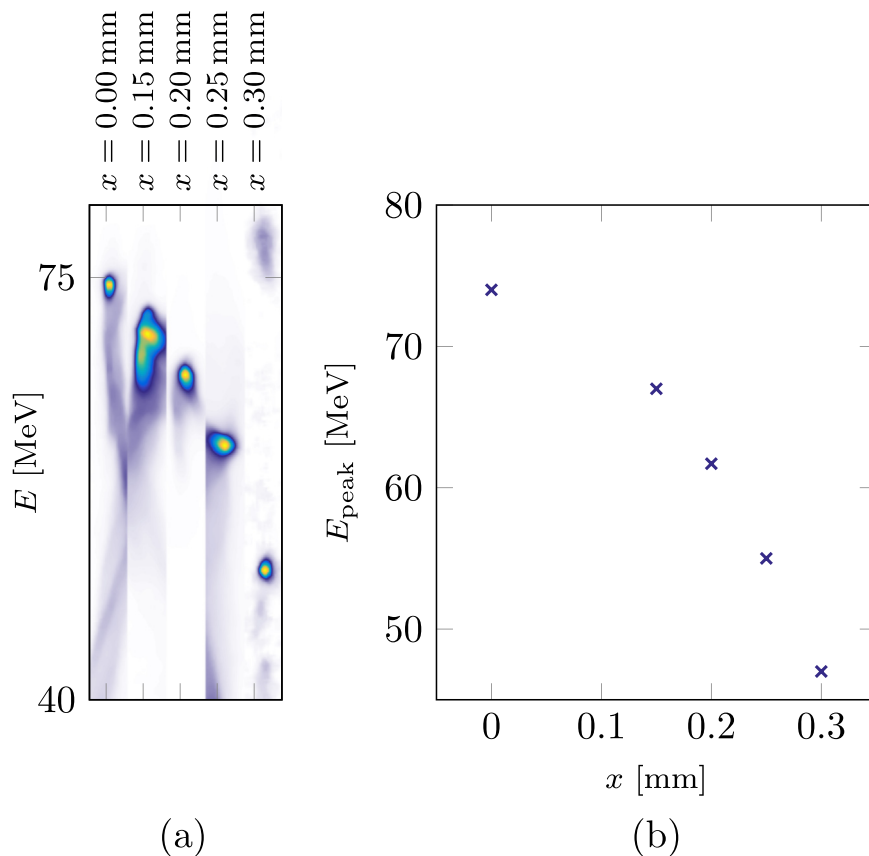
Fig. 3. The electron energy is controlled by varying the collision point in the plasma. (a) Images of the scintillating screen showing the dispersed electron beams for different collision points. (b) Corresponding peak electron energy plotted for selected points of collision. Each data point corresponds to a single shot. The peak energy decreases for collision points further back of the plasma.

focus of the main beam is expected to affect also the propagation of the main laser pulse in the plasma.

In Fig. 3(a), images of five dispersed electron beams are shown with for different collision points, x, relative to the center of the jet, tuned using method (II) of moving the gas jet. Correspondingly, the peak energy for these shots are plotted in Fig. 3(b) as a function of collision point, x. During this sequence, the $\lambda/2$ wave retarder is removed from the injection beam path and the plasma electron number density is set to 1.0×10^{19} cm^{-3}. Although the magnitude of the accelerating field is varying over during the full acceleration distance, the average, effective, accelerating field is estimated to 90 MV/mm from this figure.

4. Discussion

It is clear from the results that injection and trapping of electrons is triggered by the interaction between the two laser pulses. Furthermore, it is confirmed that the injection is triggered due to the interference between the fields of the two laser pulses, since no beams of accelerated electrons were observed with crossed polarization of the two pulses.

The experiment still suffers from large fluctuations in the resulting beams of accelerated electrons. These fluctuations most likely comes from scatter and drift of the pointing of the two beams, which was observed during the experiment on images of the scattered light from the two laser pulses as they propagate through the plasma. Although, the experimental results show that beams with low divergence and small energy spread can be achieved by this method, the experiment still suffers from large fluctuations.

5. Summary and outlook

We have demonstrated a compact set-up for the colliding pulse injection scheme for laser wakefield accelerators, by picking off part of the main laser pulse, close to the point of interaction, to trigger the injection. The colliding pulse injection scheme provides electron beams with excellent quality, regarding divergence and energy spread. The scheme also provides means to control both the electron energy and amount of charge in the beams of accelerated electrons.

Future experiments on the colliding pulse injection scheme are planned, aiming to decrease the shot-to-shot fluctuations of the beams of accelerated electrons.

References

[1] T. Tajima, J.M. Dawson, Physical Review Letters 43 (1979) 267.
[2] J. Faure, Y. Glinec, A. Pukhov, S. Kiselev, S. Gordienko, E. Lefebvre, J.-P. Rousseau, F. Burgy, V. Malka, Nature 431 (2004) 541.

[3] C.G.R. Geddes, C. Toth, J. van Tilborg, E. Esarey, C.B. Schroeder, D. Bruhwiler, C. Nieter, J. Cary, W.P. Leemans, Nature 431 (2004) 538.

[4] S.P.D. Mangles, C.D. Murphy, Z. Najmudin, A.G.R. Thomas, J.L. Collier, A. E. Dangor, E.J. Divall, P.S. Foster, J.G. Gallacher, C.J. Hooker, D.A. Jaroszynski, A. J. Langley, W.B. Mori, P.A. Norreys, F.S. Tsung, R. Viskup, B.R. Walton, K. Krushelnick, Nature 431 (2004) 535.

[5] A.J. Gonsalves, K. Nakamura, C. Lin, D. Panasenko, S. Shiraishi, T. Sokollik, C. Benedetti, C.B. Schroeder, C.G.R. Geddes, J. van Tilborg, J. Osterhoff, E. Esarey, C. Toth, W.P. Leemans, Nature Physics 7 (2011) 862.

[6] G. Golovin, S. Chen, N. Powers, C. Liu, S. Banerjee, J. Zhang, M. Zeng, Z. Sheng, D. Umstadter, Physical Review Special Topics - Accelerators and Beams 18 (2015) 011301.

[7] M. Hansson, B. Aurand, X. Davoine, H. Ekerfelt, K. Svensson, A. Persson, C.-G. Wahlström, O. Lundh, Physical Review 18 (2015) 071303.

[8] M. Burza, A. Gonoskov, K. Svensson, F. Wojda, A. Persson, M. Hansson, G. Genoud, M. Marklund, C.-G. Wahlström, O. Lundh, Physical Review Special Topics - Accelerators and Beams 16 (2013) 011301.

[9] K. Schmid, A. Buck, C.M.S. Sears, J.M. Mikhailova, R. Tautz, D. Herrmann, M. Geissler, F. Krausz, L. Veisz, Physical Review Special Topics—Accelerators and Beams 13 (2010) 091301.

[10] C. McGuffey, A.G.R. Thomas, W. Schumaker, T. Matsuoka, V. Chvykov, F. J. Dollar, G. Kalintchenko, V. Yanovsky, A. Maksimchuk, K. Krushelnick, V. Y. Bychenkov, I.V. Glazyrin, A.V. Karpeev, Physical Review Letters 104 (2010) 025004.

[11] F.G. Desforges, B.S. Paradkar, M. Hansson, J. Ju, L. Senje, T.L. Audet, A. Persson, S. Dobosz-Dufrénoy, O. Lundh, G. Maynard, P. Monot, J.-L. Vay, C.-G. Wahlström, B. Cros, Physics of Plasmas 21 (2014) 120703.

[12] E. Esarey, R.F. Hubbard, W.P. Leemans, A. Ting, P. Sprangle, Physical Review Letters 79 (1997) 2682.

[13] G. Fubiani, E. Esarey, C.B. Schroeder, W.P. Leemans, Physical Review E 70 (2004) 016402.

[14] Z.-M. Sheng, K. Mima, Y. Sentoku, M.S. Jovanović, T. Taguchi, J. Zhang, J. Meyer-ter Vehn, Physical Review Letters 88 (2002) 055004.

[15] J. Faure, C. Rechatin, A. Norlin, A. Lifschitz, Y. Glinec, V. Malka, Nature 444 (2006) 737.

[16] C. Rechatin, J. Faure, A. Ben-Ismail, J. Lim, R. Fitour, A. Specka, H. Videau, A. Tafzi, F. Burgy, V. Malka, Physical Review Letters 102 (2009) 164801.

[17] O. Lundh, J. Lim, C. Rechatin, L. Ammoura, A. Ben-Ismail, X. Davoine, G. Gallot, J.-P. Goddet, E. Lefebvre, V. Malka, J. Faure, Nature Physics 7 (2011) 219.

[18] G.R. Plateau, N.H. Matlis, C.G.R. Geddes, A.J. Gonsalves, S. Shiraishi, C. Lin, R. A. van Mourik, W.P. Leemans, Review of Scientific Instruments 81 (2010) 033108.

[19] A. Buck, K. Zeil, A. Popp, K. Schmid, A. Jochmann, S.D. Kraft, B. Hidding, T. Kudyakov, C.M.S. Sears, L. Veisz, S. Karsch, J. Pawelke, R. Sauerbrey, T. Cowan, F. Krausz, U. Schramm, Review of Scientific Instruments 81 (2010) 033301.

[20] M. Hansson, L. Senje, A. Persson, O. Lundh, C.-G. Wahlström, F.G. Desforges, J. Ju, T.L. Audet, B. Cros, S. Dobosz Dufrénoy, P. Monot, Physical Review Special Topics - Accelerators and Beams 17 (2014) 031303.